Ultrasound in Med. & Biol., Vol. 47, No. 11, pp. 3135–3146, 2021

0301-5629/$ - see front matter

https://doi.org/10.1016/j.ultrasmedbio.2021.07.012

● *Original Contribution*

FOCAL BONE-MARROW DEFECTS IN THE JAWBONE DETERMINED BY ULTRASONOGRAPHY—VALIDATION OF NEW TRANS-ALVEOLAR ULTRASOUND TECHNIQUE FOR MEASURING JAWBONE DENSITY IN 210 PARTICIPANTS

JOHANN LECHNER,* BERND ZIMMERMANN,† and MARLENE SCHMIDT‡

* Clinic for Integrative Dentistry, Munich, Germany; † Qinno, Wessling, Germany; and ‡ STEYR Motorenwerke, Ramingdorf, Austria

(*Received* 5 *May* 2020; *revised* 1 *July* 2021; *in final form* 13 *July* 2021)

Abstract—Ultrasound imaging of the jawbone is not currently used in dental medicine to determine bone density. Bone-marrow defects in the human jawbone (BMDJ/FDOJ) are widely discussed in dentistry owing to their role in implant failures and as sources of inflammation in various immune diseases. The use of through-transmission alveolar ultrasonography (TAU) to locate BMDJ/FDOJ was evaluated in this study using a new TAU apparatus (TAU-n). The objective was to determine whether TAU-n readings accurately indicate the clinical parameters to detect BMDJ/FDOJ. Three parameters were compared with TAU-n measurements: 2-D orthopantomogram, Hounsfield units using digital volume tomography and post-operatively measured levels of RANTES/CCL5 expression in BMDJ/FDOJ samples. Based on the available clinical data, Hounsfield units, RANTES/CCL5 expression and TAU-n color codes yielded consistent results with respect to bone mineral density. Thus, ultrasonography with TAU-n is a reliable and efficient diagnostic method to screen for BMDJ/FDOJ in dentistry. (E-mail: drlechner@aol.com) © 2021 The Author(s). Published by Elsevier Inc. on behalf of World Federation for Ultrasound in Medicine & Biology. This is an open access article under the CC BY-NC-ND license (http://creativecommons.org/licenses/by-nc-nd/4.0/).

Key Words: **Bone marrow defects of the jaw, Digital volume tomography, Fatty-degenerative osteolysis/osteonecrosis of the jaw, Orthopantomogram, RANTES/CCL5, TAU-n device, Transalveolar ultrasonography.**

INTRODUCTION

In the medical field, ultrasonography is widely used to image various types of soft tissues. In principle, images of structures in the body are generated by analyzing the reflection of ultrasound waves. To derive useful information concerning the status of the jawbone, different ultrasound techniques must be used, because the ultrasound waves are almost completely reflected at the interface between bone and soft tissue. *In vivo* measurement of ultrasound velocity in human cortical bone was introduced as a rapid, reliable and non-invasive method which could be used to analyze the mechanical properties of bone (Greenfield et al. 1981). Cortical bone samples show the highest values, followed by mixed bone samples and cancellous bone samples, with the latter showing the lowest values (Kumar et al. 2012). Thus, guided ultrasound waves are able to detect ischemic bone-marrow diseases—that is, focal osteoporotic defects or cavitations in the jawbone (Al-Nawas et al. 2001). Intra-oral equipment used in guided ultrasound must be minimized, however, as the area cannot be examined with commonly used ultrasound apparatus. Until now, ultrasound examinations have thus been of limited use in dental medicine, although they have been used to detect "focal" bone defects of the jawbone (focal osteoporotic marrow defects), as described in previous scientific research (Lipani et al. 1982; Kaufman and Einhorn 1993). The status of cancellous bone in the jaws may be of great clinical importance. Researchers have provided anatomical evidence that cancellous bone may be significantly degenerated, a phenomenon described as ischemic osteonecrosis leading to cavitational lesions (Bouquot et al. 1992).

We conducted an in-depth investigation of the tissue in such lesions, which appeared as clumps of fat within intact cortical bone. This tissue was in an ischemic, fatty-degenerative state. The observed bone marrow defects of the jaw (BMDJ) were thus defined as fatty-

Correspondence to: Johann Lechner, Clinic for Integrative Dentistry, Gruenwalder Str. 10A, 81547 Munich, Germany E-mail: drlechner@aol.com

degenerative osteolysis/osteonecrosis of the jawbone (FDOJ). The clumps of fat found in osteolytic jawbone are extremely biochemically active and produce specific cytokines in high amounts, the most notable of which is the chemokine RANTES (more recently known as CCL5; R/C). This chronic R/C production may influence immunologic patterns and exacerbate systemic immunologic diseases (Lechner and Mayer 2010; Lechner and von Baehr 2013, 2015; Lechner, Huesker et al. 2017; Lechner, Schuett et al. 2017). The status of cancellous bone in the jaw is of great importance with respect to dental implants and the success of implantology, according to previous publications by other authors (Klein et al. 2008; Lee et al. 2013). One of the most significant concerns associated with the treatment of this condition, however, is the fact that jawbone with fatty-degenerated bone marrow does not show signs of abnormal findings on X-ray examination (Lechner 2014). Being virtually undetectable on any type of commonly used 2-D X-ray examination, the occurrence and phenomena of BMDJ/FDOJ remain widely unknown and are even denied. To overcome this challenge, the use of through-transmission alveolar ultrasonography (TAU) was evaluated using a new TAU apparatus (TAU-n; CaviTAU, Qinno GmbH, Wessling, Germany; international patent application PCT/EP2018/084199). The CaviTAU is approved by European Union medical authorities according to MDD 93/42/EWG.

AIM AND OBJECTIVES

The aim of the present study was to evaluate BMDJ/FDOJ using TAU-n and to determine whether TAU-n measurements are practical and capable of promoting quality assurance in assessing BMDJ/FDOJ. Specifically, we aimed to answer the following questions: Are conventional radiographic techniques suitable for detecting osteolytic bone-marrow defects in the jaw (BMDJ/FDOJ), which may display local silent inflammation? Is a newly available ultrasound device (TAU-n) for radiation-free measurement of bone density suitable for visualizing the condition of BMDJ/FDOJ?

MATERIALS AND METHODS

Participant selection

All 210 participants who were enrolled in this study were seeking to uncover the etiology of their respective systemic immunologic diseases, specifically the possibility that BMDJ/FDOJ-induced "silent inflammation" of the jawbone might be involved in the pathogenesis of the disease. The samples and data were taken directly from daily clinical practice at the Clinic for Integrative Dentistry (Munich, Germany). Specifically, the data were obtained in the course of the patients' routine medical care and were retrospectively evaluated. In cases that necessitated surgical treatment, samples of BMDJ/FDOJ were evaluated post-operatively to assess the level of R/C inflammatory markers. Radiographic examinations, namely 2-D orthopantomogram (OPG) and digital volume tomography (DVT)/cone-beam computed tomography, were assessed to determine bone density and provide appropriate medical indications for the surgical treatment of BMDJ/FDOJ in these patients. This indication was supplemented by bone density measurements using TAU-n. The average age of the investigation group was 53.02 y; 129 were women and 81 were men.

The clinical case studies presented here were performed as part of a case-control study and were deemed to be retrospective in nature. Approval was granted by the accredited forensic institute, IMD-Berlin (DIN EN 15189/DIN EN 17025). All participants provided written informed consent (as outlined in the Public Library of Science consent form) to participate in this study. Patients taking bisphosphonates were excluded from the study. All participants reported that they were not taking vitamin D supplements.

PRE-OPERATIVE METHODS TO DETERMINE BONE-MARROW DEFECTS IN JAWBONE (BMDJ/FDOJ)

Determining BMDJ/FDOJ with conventional 2-D OPGs

Panoramic radiographs are routinely used in clinical dentistry. This imaging technique is inexpensive and provides a general overview of the entire jaw and a method of initial assessment of the condition of the jaw. The Orangedental PaX-i3D Duo 3D Multi X-ray unit used in this study displays a measurement of relative bone density of the jawbone (rel-JBD) in the 2-D OGP Panoramix version. A red line shows the measuring range. Figure 1 presents the results of this rel-JBD measurement: The left image shows the relative density of an all-ceramic crown at 0.9. The right image shows the relative density of a healthy area of cancellous bone at 0.49.

Determining BMDJ/FDOJ with 3-D cone-beam computed tomography/DVT

Modern X-ray methods, like DVT, allow the clinician to perform a 3-D assessment of the jawbone using Hounsfield units (HUs), which are generally scientifically recognized as a bone-density assessment tool. HUs are used to describe the attenuation of X-ray radiation in tissues, and this information is displayed in grayscale images. The HU scale ranges from −1000 (attenuation coefficient of air) to −120 (fat), +300 to +400 (healthy cancellous bone) and +1800 to +2200 (cortical bone). Water is defined as 0 HU. Recently, methods to

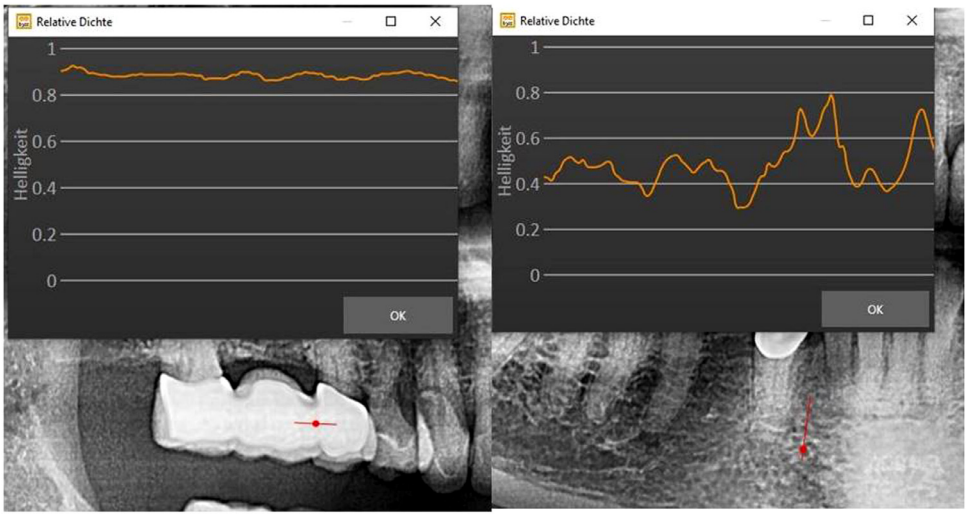

Fig. 1. Example of measurement of relative bone density using OPG. The attenuation coefficients are displayed over the entire test section as a progression curve. In the present validation, only the mean values are used. Measurement of relative jawbone density (rel-JBD) values with an Orangedental PaX-i3D Duo 3D Multi. Legend: Red lines mark the measuring range to display the relative density in the 2-D OPG. OPG = orthopantomogram.

determine HU attenuation coefficients have become available (Norton and Gamble 2001), as actual HU values can be derived using DVT (Misch 1999; Swennen and Schutyser 2006). Further investigations have classified the density of cancellous bone in the jawbone into five categories, with the poorest jawbone density below 150 HU (class 5). In this study, we used specific DVT equipment (PaX-i3D Duo 3D Multi X-ray, Orangedental, Biberach an der Riss, Germany) with the appropriate software to evaluate the density of the jawbone in HUs. In accordance with the DIN 6868-57 standard, the viewing monitors were set with a contrast >40:1 and a brightness ≥120 cd/m^2. The Orangedental PaX-i3D Duo 3D Multi X-ray machine used in this validation study showed the mean value of a randomly selected measurement path, with the maximum and minimum values presented as a progression curve (Fig. 2).

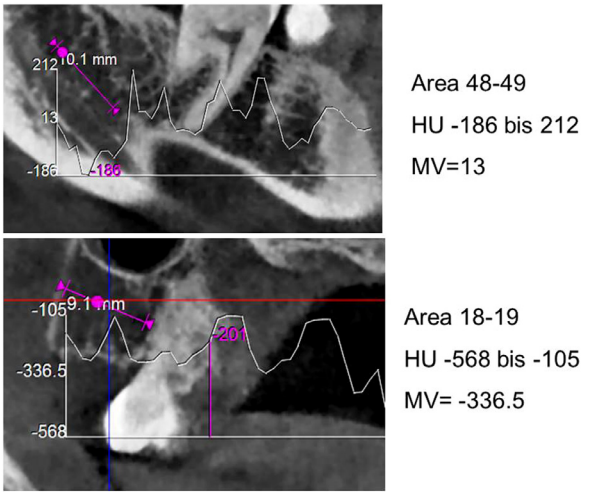

Fig. 2. Example of DVT HU measurement and evaluation of BMDJ/FDOJ. The HU attenuation coefficients are shown as a curve over the measured section. In the present validation study, only the mean values are used. BMDJ/FDOJ = bone-marrow defects of the jaw/fatty-degenerative osteolysis/osteonecrosis of the jaw; DVT = digital volume tomography; HU = Hounsfield units.

Determining BMDJ/FDOJ with TAU-n using ultrasound waves

Attenuation in the amplitude of the ultrasound wave is indicative of pathologic changes in the jawbone and depends on the properties of the medium through which the wave is propagated (Mahmoud et al. 2008). Corresponding values are based on published data from Wells (1999) and Njeh et al. (1999). TAU-n generates an ultrasound wave and passes that wave through the jawbone. This wave is produced by an extra-oral transmitter and then detected and measured by a receiving unit that is positioned intra-orally. Both parts (the transmitter and receiving unit) are fixed in a parallel position using a single handpiece. The size of the TAU-n receiving unit is configured such that it can be easily placed inside the mouth of a patient. TAU-n uses 91 piezoelectric elements that are arranged hexagonally. The jawbone must be positioned between the two parts of the measuring unit. With respect to the parts of the measuring unit to be placed inside a patient's mouth, the acoustical coupling between those parts and the alveolar ridge is performed with the aid of a semi-solid gel (Qinno). The contact between the jawbone and both the extra-oral ultrasound

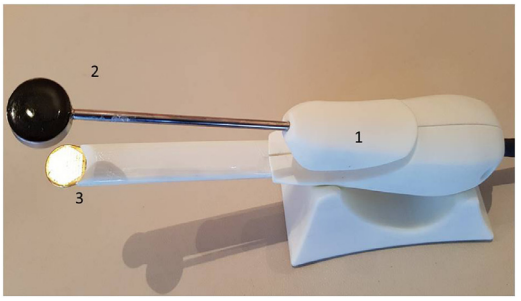

Fig. 3. Coplanar and fixed arrangement of the transmitter and receiver: (1) Handpiece with an ultrasound sender and receiver unit connected to a computer and screen. (2) Ultrasound transmitter. (3) Ultrasound receiver with 91 piezoelectric elements.

transmitter and intra-oral ultrasound receiver (Fig. 3) is optimized and individualized using a special ultrasound gel cushion that was developed for this purpose. The results are shown on a color monitor that displays different colors depending on the degree of attenuation. A semi-solid, single-use gel pad is used around the receiver for hygienic reasons (Fig. 4).

Color scale associated with TAU-n attenuation coefficients

Figure 5 presents the color scheme associated with the TAU-n attenuation coefficients. This scheme corresponds to an ultrasound signal-strength scale (top bar) and a color scale indicating the different degrees of bone density (lower bar). This color scale shows that the colors used to indicate different densities each represent a small part of the entire signal range. Logarithmic averaging broadens the range of bone-density measurements and increases the size of the area in green.

The representations of the measurements provided by the color-coding scheme are concerned with two functions. With the red/green color scale, the bone in the medically relevant area of conspicuousness is shown. The second color-coded scale shows structural differences, which serves as an orientation aid for the user in the placement of the measuring receiver. In this way, the orientation and position of the receiver may be monitored (via live display) while the measurement position is slowly adjusted before the relevant area is captured and stored.

The TAU-n display

The TAU-n display is able to capture the following physical structures in the dentoalveolar region (Fig. 6), with corresponding color variations of 91 color columns/cm^2: solid bone in the marginal cortical area (green or white/light blue); healthy medullary cancellous bone (green or white/light blue); chronic inflammatory medullary cancellous bone with fatty-degenerative components (red or black/dark blue); fatty nerve structures (yellow/light blue); and extremely dense and complex structures such as teeth, implants and crowns (green or white/light blue).

Numerical representation of TAU-n attenuation coefficients

The TAU-n software numerically represents the attenuation coefficients of the TAU-n measurement range. By a mouse click on one of the 91 sensor fields of a given measurement, the software marks the field and displays the measured value in a logarithmic evaluation. The sensor fields that show the highest attenuation values defined by TAU-n are marked in either red or black, and this indicates the bone density of an area of BMDJ/FDOJ. TAU-n computes the logarithmic average of the sum of the sensor elements with the lowest density unit as Average(log), displayed in red (Fig. 7, left panel). In the same way, the logarithmic average of the sensor elements with the highest density—equivalent to reduced attenuation by solid structures—is displayed in

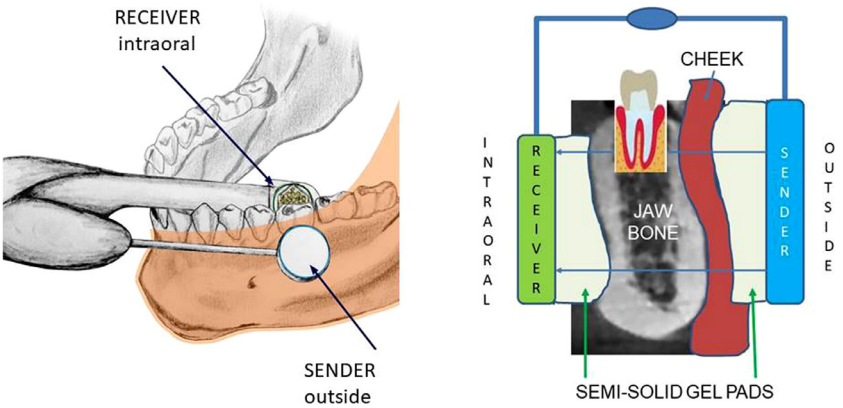

Fig. 4. Left: Positioning of the transmitter (*outside*) and receiver (*intra-oral*) in the lower jaw; the shaded area marks the cheek. Right: The transmitter (*in blue on the right*) and receiver (*in green on the left*) are in a fixed coplanar position (*a blue bar connects them*); semi-solid gel pads between the transmitter and the cheek on the outside of the mouth and between the receiver and the alveolar ridge in the intra-oral position; trans-alveolar ultrasonic impulse from the transmitter to the receiver (*blue arrows*).

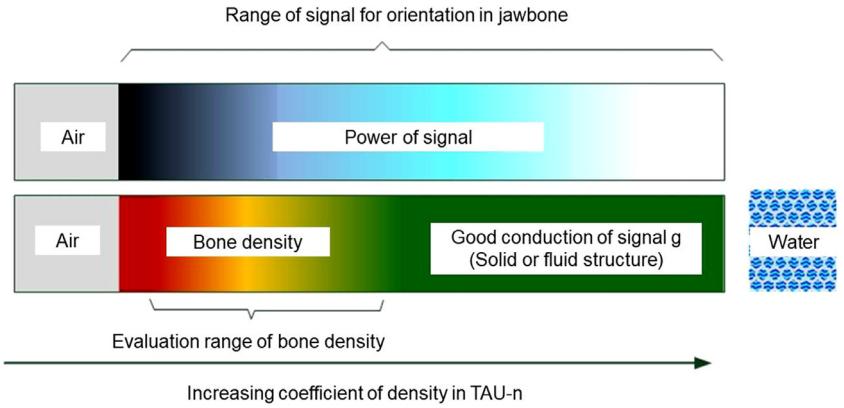

Fig. 5. The color scale is used by the TAU-n device to indicate different degrees of density; gray corresponds to air (*i.e.,* the far left of the scale), and blue area corresponds to water (*i.e.,* the far right of the scale). The signal strength received by the sensor (*top bar*) is displayed in blue and increases from dark to light with increasing density coefficients. Bone density (*lower bar*) is indicated by a color scale ranging from red to green, representing high attenuation of diminished bone density (*red*) and reduced attenuation with increasing density (*green*). TAU-n = new through-transmission alveolar ultrasonography.

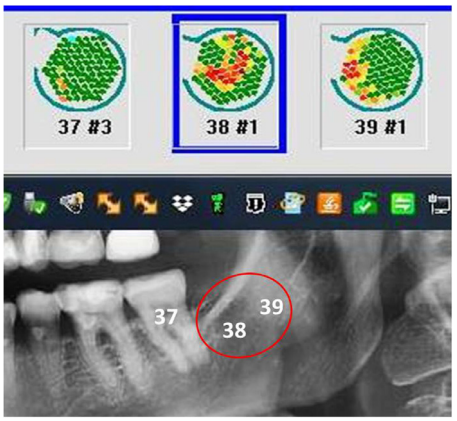

Fig. 6. Example of the color-coding scheme associated with attenuation used by TAU-n in area 38. In the upper panel, the measurement of jaw areas 37 to 38/39 (*i.e.,* the retromolar area) is presented. TAU-n displays different degrees of mineralization, as highlighted by the various color patterns of 91 individual sensor fields that correspond to each jawbone area. Green indicates hard and dense structures that correspond to a higher degree of mineralization in spongial jawbone or cortical bone; it also denotes teeth, dental crowns or implants. Yellow indicates diminished bone density and also corresponds to the nerve canal in the lower jaw. Red indicates severely diminished bone density with a low degree of mineralization, corresponding to BMDJ/FDOJ areas. BMDJ/FDOJ = bone-marrow defects of the jaw/fatty-degenerative osteolysis/osteonecrosis of the jaw; TAU-n = new through-transmission alveolar ultrasonography.

green (Fig. 7, right panel). In the following sections and Table 1, the term "TAU-n log" is used to represent the values of Average(log) displayed by TAU-n.

Problems of acoustic coupling in TAU-n

Practical application of the transducer and receiver with fixed geometric positions to obtain intra-oral ultrasonic measurements (*i.e.,* within the mouth of a patient) with sufficient acoustical conductivity proved difficult. The ultrasonic gel, which was placed inside the patient's mouth, was shown to be the main obstacle in attempting to obtain signals from TAU-n in an easy and reproducible manner. The primary difficulty is ensuring that the ultrasonic gel is completely free of air bubbles, given its high viscosity. Air bubbles interfere with obtaining reliable and repeatable measurements. In addition, we found that the anatomical contour of the jawbone at the site of measurement and the plane surface of the intra-oral receiver did not adequately conform to one

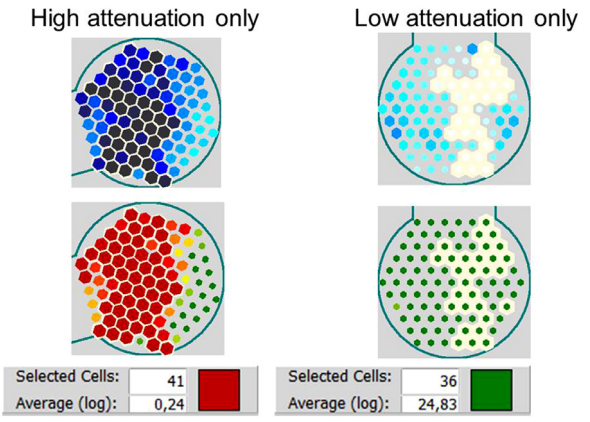

Fig. 7. Sensor elements. Numerical representation of the TAU-n attenuation coefficients for diminished bone density (*left*) and for dense material (*right*). Selected sensor cells (left panel: high attenuation; right panel: low attenuation) are indicated by a white border. The evaluation is presented in the window beneath for a number of selected sensor cells; the result is displayed as a logarithmic mean, which is associated with a corresponding color (*i.e.,* left: *red* = high attenuation; right: *green* = corresponds to low attenuation). TAU-n = new through-transmission alveolar ultrasonography.

Table 1. The four values measured to assess BMDJ/FDOJ

Participant	OPG	HU	Average (log)	R/C (pg/mL)
1	0.6	−29.0	1.35	8212.50
2	0.4	−96.0	1.41	2762.50
3	0.7	−533.0	0.67	5700.00
4	0.75	−326.0	4.49	3250.00
5	0.3	−316.0	0.3	3925.00
6	0.5	−591.0	0.33	3762.50
7	0.6	−295.0	0.36	2162.50
8	0.4	−93.0	0.44	2187.50
9	0.4	−250.0	0.84	2850.00
10	0.65	−745.0	1.58	722.50
11	0.55	−263.0	0.84	1825.00
12	0.5	−311.0	0.46	1787.50
13	0.45	89.0	0.67	1725.00
14	0.4	−300.0	1.37	5387.50
15	0.45	−340.0	0.87	992.50
16	0.5	−306.5	1.04	2512.50
17	0.3	−228.5	0.82	2362.50
18	0.65	11.5	0.9	3862.50
19	0.6	−58.5	0.64	457.50
20	0.5	−659.0	0.85	873.75
21	0.35	−447.0	0.31	706.25
22	0.4	−431.0	0.83	2825.00
23	0.4	−31.5	0.64	1165.00
24	0.55	−450.0	1.12	405.00
25	0.45	−565.0	0.69	146.25
26	0.4	−68.0	0.72	766.25
27	0.55	−647.0	2.58	5525.00
28	0.5	54.5	1.52	7275.00
29	0.6	−549.0	0.82	2112.50
30	0.4	−130.0	0.76	2575.00
31	0.65	120.5	0.94	5562.50
32	0.7	−345.0	0.95	1612.50
33	0.6	−77.5	0.58	205.00
34	0.65	72.5	1.85	2962.50
35	0.55	−173.0	1.07	1875.00
36	0.5	−249.0	0.66	267.50
37	0.4	−413.0	0.38	1750.00
38	0.7	−291.0	0.52	1887.50
39	0.6	−238.5	1.32	2000.00
40	0.6	−537.0	1.22	1337.50
41	0.65	−676.0	0.79	702.50
42	0.4	−62.0	0.54	846.25
43	0.4	−179.5	2.58	408.75
44	0.6	−243.0	1.26	810.00
45	0.4	−560.0	1.5	518.75
46	0.6	−494.0	0.84	486.25
47	0.55	−387.0	0.75	2875.00
48	0.6	−379.0	1.14	2737.50
49	0.4	−228.0	0.32	2425.00
50	0.5	−440.0	0.68	1078.75
51	0.6	−308.0	0.54	1800.00
52	0.6	−322.0	1.21	19,125.00
53	0.5	−589.0	2.29	645.00
54	0.55	−518.0	1.21	1575.00
55	0.45	−294.0	0.51	2187.50
56	0.55	−671.0	0.89	767.50
57	0.55	−244.0	1.89	580.00
58	0.3	−573.0	1.77	8062.50
59	0.65	−454.0	0.93	910.00
60	0.4	99.0	1.57	5025.00
61	0.2	−182.5	1.78	4562.50
62	0.6	−335.0	1.03	3725.00
63	0.4	−288.0	0.79	3587.50
64	0.5	−132.0	1.75	840.00
65	0.6	−202.0	1.03	2300.00
66	0.3	−418.0	0.81	5362.50
67	0.45	−290.0	1.38	1637.50
68	0.6	−41.0	0.96	636.25
69	0.4	−184.0	1.67	2200.00
70	0.5	−227.0	1.11	863.75
71	0.6	−198.0	1.38	1587.50
72	0.45	−261.0	1.65	3987.50
73	0.55	−543.0	1.01	3937.50
74	0.6	−363.0	1.19	1275.00
75	0.45	−268.0	0.32	10,150.00
76	0.55	−110.0	1.69	573.75
77	0.75	−248.0	1.61	1337.50
78	0.65	−142.0	1.28	611.25
79	0.35	−264.0	2.51	893.75
80	0.45	−301.0	0.86	2100.00
81	0.5	−654.0	1.05	866.25
82	0.75	−168.0	1.53	1775.00
83	0.4	146.0	0.79	1400.00
84	0.4	123.0	1.37	1800.00
85	0.4	−222.0	0.77	1925.00
86	0.6	−36.0	1.23	303.75
87	0.4	−5.0	1.15	1215.00
88	0.25	−213.0	1.52	412.50
89	0.5	88.0	1.24	495.00
90	0.25	−347.0	1.19	1600.00
91	0.45	45.0	1	1725.00
92	0.4	−38.0	0.47	527.50
93	0.5	160.0	1.28	3612.50
94	0.5	−313.0	0.82	1337.50
95	0.55	119.0	1.38	1192.50
96	0.4	−196.0	0.8	1246.25
97	0.55	−17.0	0.96	638.75
98	0.3	−457.0	0.47	6512.50
99	0.3	−373.0	0.7	456.25
100	0.5	−209.0	1.25	3275.00
101	0.4	−438.0	0.81	2262.50
102	0.5	−38.0	0.88	447.50
103	0.45	−404.0	0.47	746.25
104	0.35	−170.0	1.64	1400.00
105	0.4	126.0	1.07	436.25
106	0.55	103.0	1.05	588.75
107	0.4	96.0	0.84	1312.50
108	0.7	162.0	0.97	1500.00
109	0.6	−66.0	1.12	223.75
110	0.45	−105.0	1.21	373.75
111	0.5	−20.0	0.98	277.50
112	0.5	−208.0	1.58	705.00
113	0.6	−264.0	1.8	1912.50
114	0.6	−83.0	0.81	3962.50
115	0.6	−38.0	0.67	432.50
116	0.4	−348.0	1.33	1675.00
117	0.4	150.0	1.17	311.25
118	0.4	−166.0	1.35	1023.75
119	0.55	144.0	1.37	996.25
120	0.45	−94.0	1.71	498.75
121	0.5	41.0	2.67	3187.50
122	0.5	−157.0	1.4	417.50
123	0.45	−291.0	0.61	1325.00
124	0.6	77.0	1.17	917.50
125	0.35	−96.0	1.89	1687.50
126	0.4	4.0	0.98	228.75
127	0.25	−183.0	1.58	355.00
128	0.45	−43.0	1.18	407.50
129	0.4	−147.0	0.36	541.25
130	0.4	−145.0	0.73	408.75
131	0.4	−245.0	0.73	572.50

(*continued*)

Table 1 (***Continued***)

(*continued*)

Table 1 (***Continued***)

Participant	OPG	HU	Average (log)	R/C (pg/mL)
132	0.65	150.0	1.24	1600.00
133	0.4	−87.0	1.59	586.25
134	0.2	−138.0	1.38	1287.50
135	0.5	−27.0	1.09	945.00
136	0.35	−257.0	1.22	647.50
137	0.35	−120.0	0.31	267.50
138	0.35	−116.0	0.95	233.75
139	0.55	−30.0	1.38	572.50
140	0.4	150.0	1.57	673.75
141	0.6	−155.0	1.12	2862.50
142	0.55	157.0	1.11	691.25
143	0.5	−127.0	0.67	1650.00
144	0.3	−110.0	0.93	565.00
145	0.55	84.0	0.84	1137.50
146	0.45	−414.0	0.87	8087.50
147	0.45	−122.0	1.53	1217.50
148	0.4	−145.0	1.5	4075.00
149	0.6	170.0	0.67	562.50
150	0.5	97.0	0.97	1337.50
151	0.45	197.0	0.5	1875.00
152	0.6	−117.0	1.6	950.00
153	0.4	−363.0	1.95	1111.25
154	0.35	16.0	1.26	4437.50
155	0.55	−123.0	0.76	2750.00
156	0.4	23.0	1.58	370.00
157	0.35	52.0	1.48	370.00
158	0.35	320.0	0.58	518.75
159	0.4	−108.0	0.36	1475.00
160	0.6	−23.0	1.04	5175.00
161	0.4	−566.0	1.26	873.75
162	0.5	−55.0	1.28	2637.50
163	0.45	−305.0	0.85	486.25
164	0.5	93.0	1.9	460.00
165	0.55	42.0	0.75	457.50
166	0.5	59.0	1.46	1312.50
167	0.5	−175.0	0.96	5462.50
168	0.4	−450.0	1.07	11,437.50
169	0.5	107.0	1.66	1163.75
170	0.45	−8.0	1.86	650.00
171	0.6	192.0	1.56	1300.00
172	0.35	43.0	0.62	573.75
173	0.45	−120.0	0.73	190.00
174	0.6	−96.0	1.35	966.25
175	0.55	−58.0	1.09	3137.50
176	0.25	−69.0	0.77	3225.00
177	0.5	−420.0	0.94	978.75
178	0.4	−225.0	0.84	2675.00
179	0.35	123.0	0.89	2287.50
180	0.6	−115.0	0.7	1825.00
181	0.3	−63.0	1.31	1250.00
182	0.4	−175.0	1.57	1108.75
183	0.6	97.0	1.79	1425.00
184	0.5	2.0	1.56	1750.00
185	0.55	179.0	1.5	647.50
186	0.45	40.0	1.89	968.75
187	0.4	65.0	0.67	733.75
188	0.7	200.0	1.41	555.00
189	0.5	−44.0	1.23	1950.00
190	0.35	−58.0	1.44	631.25
191	0.4	−116.0	1.34	2362.50
192	0.35	−293.0	1.28	338.75
193	0.35	153.0	0.71	985.00
194	0.5	−316.0	1.32	1600.00
195	0.2	−231.0	0.35	4574.00
196	0.5	−162.0	1.09	3400.00
197	0.4	−94.0	0.73	1675.00
198	0.6	167.0	1.89	370.00
199	0.45	−62.0	1.25	324.00
200	0.55	−327.0	1.01	1132.00
201	0.6	−210.0	1.02	863.00
202	0.35	−197.0	1.42	2350.00
203	0.5	−550.0	1.88	1850.00
204	0.6	−290.0	0.32	863.00
205	0.5	−68.0	1.22	2887.00
206	0.3	−192.0	1.48	7912.00
207	0.5	63.0	1.56	1625.00
208	0.5	37.0	1.1	2237.00
209	0.45	−57.0	1.28	950.00
210	0.6	−154.0	0.73	661.00
	0.48	**−165.7**	**1.2**	**1950.38**

BMDJ/FDOJ = bone-marrow defects of the jaw/fatty-degenerative osteolysis/osteonecrosis of the jaw; DVT = digital volume tomography; HU = Hounsfield units; OPG = orthopantomogram; R/C = RANTES/CCL5; TAU-n = new through-transmission alveolar ultrasonography.

The mean value obtained pre-operatively for 2-D OPG was a relative bone density of 0.48; for 3-D DVT HU the value was −165.7 (normal ≥ 300), and for CaviTAU Average(log) the value was 1.2 (normal bone density > 2.0). For R/C expression, the mean was 1950.38 pg/mL (normal = 149.9 pg/mL). Pre-operative HU attenuation coefficients and corresponding TAU-n attenuation coefficients (Average(log); columns in gray) are compared with postoperatively measured levels of R/C expression from the samples obtained during surgical treatment for BMDJ/FDOJ (columns in blue). MV refers to the medium values obtained in the course of our research, and the final row compares the corresponding values of healthy jawbone found in the literature (HUs; Guglielmi and de Terlizzi 2009; Mah et al. 2010; Komar et al. 2019) and R/C levels (pg/mL; Klein et al. 2008; Lechner and Mayer 2010; Lechner and von Baehr 2013, 2015; Lechner, Huesker et al. 2017; Lechner, Schuett et al. 2017).

another. The distance between the surfaces of the receiver and the alveolar ridge was shown to vary widely.

As a solution, a semi-solid gel pad was placed between the receiver and the alveolar ridge of the patient. The sound velocity in the gel used should fall within the same range as that of soft tissue (*i.e.,* 1460−1615 m/s) and the gel should have a sound attenuation ranging from 0.3−1.5 dB/cm (1 MHz), so as not to impede the acoustical measurements in the jawbone. The haul-off speed for spontaneous resilience should not exceed 80 mm/s. The semi-solid property of the gel prevents it from evaporating or disappearing before or during measurement. To perform the measurements, inside the gel pad is a small pocket into which the receiver can be inserted. Following the elimination of any air bubbles between the receiver and the semi-solid gel, the measuring unit is ready for use.

Calibration of the TAU-n

The arrangement of the measuring unit in a defined geometry allows for easy calibration of the TAU-n. This functional test is performed with flexible gel pads covering both the transmitter and the receiver. Figure 8 illustrates the procedure—the full immersion of both parts into a vessel

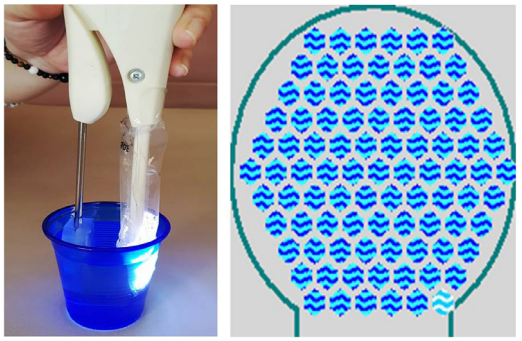

Fig. 8. Water test for calibration. Left: Transmitter and receiver must be completely submerged in water. Right: All sensor elements show watermarks with the exception of the lower right sensor element.

filled with water. The complete acoustic coupling is visible when all sensor elements show the watermark in the left image of the sensor on the computer display. This calibration in a water bath at constant conditions allows for compensation of possible deviation of the elements as a starting point for measurement. The calibration test ensures that no air pockets interfere in the arrangement of cushions, gel and sleeves and that no failure of elements or components leads to misinterpretation.

POST-OPERATIVE METHOD FOR DETERMINING BMDJ/FDOJ

Determining BMDJ/FDOJ with R/C expression

BMDJ/FDOJ cavitations contain degenerated adipocytes that exhibit a particular expression profile of the chemokine R/C (Lechner and Mayer 2010; Lechner and von Baehr 2013, 2015; Lechner, Huesker et al. 2017; Lechner, Schuett et al. 2017). Hence, BMDJ/FDOJ samples were also analyzed for expression of the inflammatory immune mediator R/C. Laboratory procedures used to define R/C expression levels in healthy jawbone and in BMDJ/FDOJ have been previously published; healthy jawbone showed R/C expression levels of 149 pg/mL, whereas a significant number of BMDJ/FDOJ samples (n = 301) among people with chronic disease (average age: 54.05 y; age range: 23−75 y; gender ratio: 89 women to 225 men) showed a 20-fold increase in R/C expression of 2940 pg/mL (Lechner and Mayer 2010; Lechner and von Baehr 2013, 2015; Lechner, Huesker et al. 2017; Lechner, Schuett et al. 2017). BMDJ/FDOJ is the only bone resorption process that shows R/C overexpression (Lechner et al. 2018). BMDJ/FDOJ also displays a reduction in expression of tumor necrosis factor-α and interleukin-6, whereas all other bone resorption-related diseases are characterized by overexpression of tumor necrosis factor-α and interleukin-6. In summary, the recent literature has shown that BMDJ/FDOJ not only is characterized by reduced mineralization and diminished bone density but also plays an important role in osteoimmunologic processes. Thus, R/C overexpression alone is involved in the characteristic and bone-degrading aspect of BMDJ/FDOJ (Lechner et al. 2018).

Based on findings in the literature (Lechner and Mayer 2010; Lechner and von Baehr 2013, 2015; Lechner, Huesker et al. 2017; Lechner, Schuett et al. 2017), it is known that an R/C expression level higher than 149 pg/mL indicates the presence of osteonecrosis or osteolysis which has resulted in diminished jawbone density. A control group of 19 participants volunteered to provide samples of healthy jawbone, which were removed using drill cores during dental implantation surgery. The inclusion criteria for this group were as follows: absence of distinctive radiologic features in 2-D OPG and 3-D DVT and inconspicuous TAU-n measurements of bone density in the implantation area. The use of bisphosphonate medication was the central exclusion criterion. The demographic data for the 19 participants in the BMDJ/FDOJ control group were average age, 51.4 y; age range, 33−72 y; gender breakdown, 10 women, 9 men.

Collection of pre-operative rel-JBD, HU and TAU-n values and post-operatively measured levels of R/C expression

In this study, a cohort of 210 participants who exhibited clinical evidence of BMDJ/FDOJ (*i.e.,* HU value, local R/C expression profile and TAU-n measurements) was identified

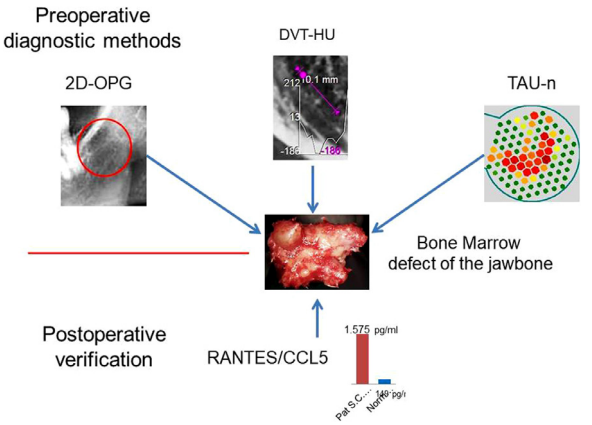

Fig. 9. The possible methods used to localize BMDJ/FDOJ. Pre-operative 2-D OPG is insufficient, but DVT with the possibility of HU measurement may provide a clear indication of BMDJ/FDOJ. The use of TAU-n as a novel, radiation-free measurement option is evaluated in this article. Post-operative multiplex analysis shows extreme R/C overexpression, providing evidence of inflammation. BMDJ/FDOJ = bone-marrow defects of the jaw/fatty-degenerative osteolysis/osteonecrosis of the jaw; DVT = digital volume tomography; HU = Hounsfield units; OPG = orthopantomogram; R/C = RANTES/CCL5; TAU-n = new through-transmission alveolar ultrasonography.

to investigate our research objective in a clinical setting. The schematic representation in Figure 9 illustrates the four validation parameters discussed and used in this study. Each of the participants in this group was assessed with TAU-n. To be included in this group, each participant was required to have the following with respect to the area of BMDJ/FDOJ investigated: positive pre-operative TAU-n measurements, low bone density (in HU values) and a post-operative evaluation of R/C expression. We compared the pre-operative TAU-n and HU values of the research group with the post-operatively obtained laboratory results of R/C expression of the corresponding jawbone areas of BMDJ/FDOJ.

Statistical analysis

The statistical analysis was conducted using the statistical software R version 3.5.1. The similarity between the HU and TAU-n methods was verified by means of the Spearman correlation coefficient.

RESULTS

Comparison of pre-operative TAU-n and HU values with post-operative evaluation of R/C expression

After evaluating the detection of BMDJ/FDOJ using TAU-n, we established clinical evidence of the TAU-n attenuation coefficients by comparing and verifying pre-operative HU and TAU-n values with the post-operatively determined R/C expression levels of corresponding BMDJ/FDOJ areas. The results are shown in Table 1. In Figure 9, we present three pre-operative methods and one post-operative method used to assess BMDJ/FDOJ. For this group of 210 participants, we carried out each of these four methods and compared the results, *i.e.,* (A) the OPG bone density; (B) the preoperative HU attenuation coefficients; (C) the corresponding TAU-n attenuation coefficients of BMDJ/FDOJ according to Average(log) in the TAU-n software (TAU-n Log in Table 1 = Average (log); see Fig. 7); and (D) the R/C expression levels in the fatty degenerated samples obtained during BMDJ/FDOJ surgery (Table 1).

Comparison of rel-JBD, HU and TAU-n values of healthy jawbone

To ensure that TAU-n generates significantly higher attenuation values in jawbone where BMDJ/FDOJ is not present, we measured rel-JBD, HU and TAU-n values in healthy jawbone. To obtain valid negative results, we focused on bone-marrow areas beneath healthy molar teeth. The process of determining rel-JBD and HU was already shown in Figure 1. The results obtained for healthy jawbone in 10 participants are presented in Table 2. We were unable to measure R/C values, because surgical intervention in areas of healthy jawbone was not possible for ethical reasons.

Table 2. Measurement of rel-JBD, HU and TAU-n values in healthy jawbone

Participant	Area	OPG	HU	TAU
1	37	0.55	272	7.02
2	37	0.5	599	8.49
3	47	0.55	97	4.46
4	37	0.45	193	7.14
5	36	0.55	678	6.89
6	37	0.45	271	11.51
7	36	0.35	744	6.71
8	46	0.6	306	10.51
9	47	0.4	329	6.16
10	37	0.4	315	9.79
Mean		0.48	380.4	7.868

HU = Hounsfield units; OPG = orthopantomogram; OPG: rel-JBD = relative bone density of the jawbone; TAU-n = new through-transmission alveolar ultrasonography.

Comparison of rel-JBD, HU and TAU-n values of healthy jawbone and BMDJ/FDOJ areas

The bone densities measured in healthy jawbone and BMDJ/FDOJ areas are compared as mean values. There is clear agreement in the rel-JBD values obtained with 2-D OPG (4.8 BMDJ/FDOJ, 4.8 healthy), whereas the HU values (−165 BMDJ/FDOJ, 380 healthy) and particularly TAU-n values (1.2 BMDJ/FDOJ, 7.8 healthy) differ significantly (Fig. 10).

DISCUSSION

Bone-marrow defects and 2-D OPG

To compare the results documented in Table 1 in terms of their clinical significance, we calculated 10 mean values of jawbone density measurements obtained with 2-D OPG from three different dental colleagues

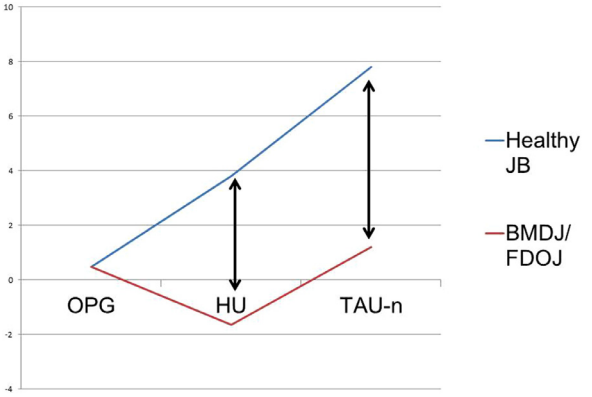

Fig. 10. Comparison of relative bone-density values determined with 2-D OPG, attenuation coefficients in HUs (1:100) and TAU-n values in healthy and BMDJ/FDOJ cohorts. BMDJ/FDOJ = bone-marrow defects of the jaw/fatty-degenerative osteolysis/osteonecrosis of the jaw; HU = Hounsfield units; OPG = orthopantomogram; TAU-n = new through-transmission alveolar ultrasonography.

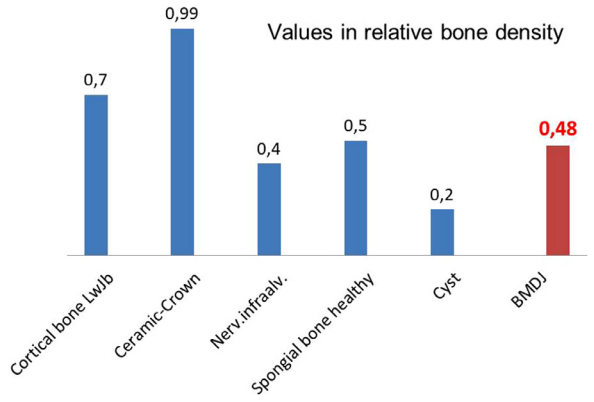

Fig. 11. Comparison of various density values with BMDJ/FDOJ values obtained using 2-D OPG. This shows that normal bone density measured in healthy spongial cancellous bone structure with a value of 0.5 is only slightly denser than the mean value of the 210 BMDJ/FDOJ areas we examine, with a medium value of 0.48. This explains in part why there is widespread doubt among dentists in the discussion about the actual existence of BMDJ/FDOJ. In summary, a critical detection of medullary bone density in BMDJ/FDOJ areas is not possible with 2-D OPG (Lechner 2014). BMDJ/FDOJ = bone-marrow defects of the jaw/fatty-degenerative osteolysis/osteonecrosis of the jaw; OPG = orthopantomogram.

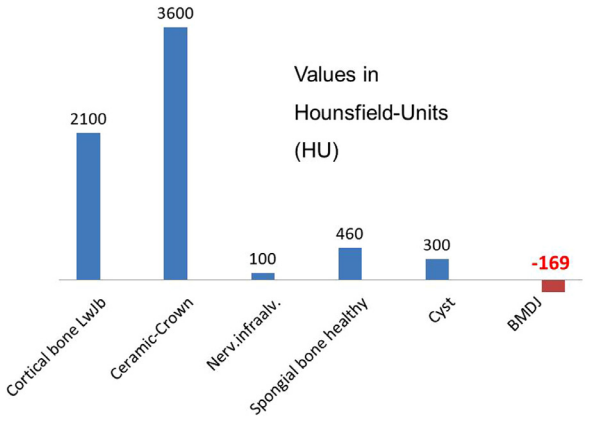

Fig. 12. Comparison of a wide variety of density values with BMDJ/FDOJ values obtained with 3-D DVT. This shows that the HU value of −169 produced by the reduced X-ray attenuation in the softened BMDJ/FDOJ areas is significantly less than the minimum value of 300 reported as healthy in the literature. A reliable assessment of the medullary bone density in areas of BMDJ/FDOJ is possible with the HU values derived using high-quality 3-D DVT (Loubele et al. 2009; Roberts et al. 2009). However, this method of examination requires a relatively high radiation exposure. Furthermore, DVT devices which provide the necessary HU measurement are costly. In our experience, inexpensive DVT units fail to achieve the requisite quality and lead to incorrect assessments based on purely subjective evaluation. BMDJ/FDOJ = bone-marrow defects of the jaw/fatty-degenerative osteolysis/osteonecrosis of the jaw; DVT = digital volume tomography; HU = Hounsfield units.

with available radiographs. The five control parameters comprised the following measurements: cortical bone on the mandibular branch, all-ceramic crown, the canal of the infra-alveolar nerve, cancellous bone normal, and cyst lumen. Figure 11 shows these values in blue. Bone-density values in areas of BMDJ/FDOJ collected from the cohort of 210 participants are presented in red.

Bone-marrow defects and 3-D DVT

As with the 2-D OPG radiographs, to compare the results documented in Table 1 in terms of their clinical significance we calculated 10 mean values of 3-D DVT measurements from three different dental colleagues with existing radiographs as before. Figure 12 shows these HU values in blue. The bone-density value of −169 HUs in the BMDJ/FDOJ areas collected from the cohort of 210 participants is presented in red.

Bone-marrow defects and TAU-n

When the TAU-n Average(log) values are compared with the DVT HU values determined in this study, both correspond to reduced bone density, which implies the presence of BMDJ/FDOJ. Further, the general correlation of HU and R/C multiplex analysis with the Average(log) values generated using the TAU-n software may be confirmed. In previous publications, light microscopy has also confirmed the reduction of bone density determined by the CaviTAU Average(log) values (Lechner et al. 2020).

The threshold for which TAU-n log indicates BMDJ/FDOJ

As shown in Table 1, the mean value of 210 TAU-n measurements in BMDJ/FDOJ areas is 1.2, with a range of 0.3 (#5) to 1.95 (#153). Accordingly, we defined the threshold for which a TAU-n log indicates diminished bone density corresponding to a BMDJ/FDOJ area at a TAU-n value of 2. TAU-n values of 4.49, 2.29 and 2.67 (participants 4, 53 and 123) were the only measurements determined beyond this threshold of 2; however, a 20-fold, 4-fold and 10-fold overexpression of R/C was also detected in these cases.

R/C expression in BMDJ/FDOJ

The values of R/C expression in the BMDJ/FDOJ samples analyzed post-operatively with multiplex methods in the laboratory average 1950.38 pg/mL, which is 13 times the normal value of 149.9 pg/mL found in healthy jawbone that we have previously published (Lechner and von Baehr 2013). First and foremost, the application of TAU-n allows for the use of low radiation levels in the stress-free detection of mineralization and metabolic disorders in the medullary region of the jawbone. Medical devices that aim to measure specific phenomena must be able to consistently reproduce their

results. In this respect, the measurements obtained with TAU-n are reliable and primarily free of operator error, as the TAU-n transmitter and receiver are positioned along a coplanar axis in a fixed arrangement. This ensures the necessary independence from the operator and the reproducibility of TAU-n measurements. Errors in acoustic coupling are avoided by displaying a gray sensor field, which is not associated with ultrasound transmission during the measurement process.

Limits in the comparability of the measured HU and TAU-n values

A 1:1 correlation of the measured values obtained with DVT in HUs and using TAU-n is not possible because both examination methods are physically different and thus measure different distances in the jaw. However, a general technical correlation may be made as follows: The measured HU values correspond to a selected cross-sectional slice of the jaw, whereas TAU-n penetrates through the entire distance from the transmitter to the sensor and thus reproduces the typical reflective and scattering properties of ultrasound. TAU-n is therefore unable to isolate particular sections within the jawbone. Furthermore, the attenuation coefficients of both methods behave in completely opposite ways. With HUs, the denser the irradiated object, the greater the positive attenuation coefficients and the lower the transmission. With TAU-n, the greater the density of the object to be examined, the lower the attenuation coefficients and, thus, the greater the sound transmission. A relationship between the two methods can still be established, however, as conspicuous areas assessed using HUs are also detectable with TAU-n and *vice versa*. To ensure that TAU-n is a reliable indicator of poor bone quality, this approach should be validated in people without BMDJ/FDOJ. Here we face an ethical obstacle, as people with HU values >300 and TAU-n log >2 are inappropriate candidates for jawbone surgery. Thus it is not possible to obtain R/C values in such cases. The study design we used is thus unable to fully answer the initial question posed in this study.

SUMMARY

The interest in the application of TAU-n lies in the decrease in bone density in BMDJ/FDOJ owing to osteolysis. The upper limit of DVT HU values of interest with respect to BMDJ/FDOJ is +300, as at this point there is a transition to healthy cancellous bone. Values over +300 HUs thus fall outside the necessary detection range of TAU-n. The HU values produced in this study (range: −680 to +150) indicate BMDJ/FDOJ in class 5 cases (Mah et al. 2010). The data presented here show that HU values demonstrate osteolysis and correspond to R/C overexpression in BMDJ/FDOJ areas (Lechner et al. 2018). When the data derived from both methods used to evaluate BMDJ/FDOJ (*i.e.,* HU values and R/C expression) are compared with the TAU-n results, there is a correlation between the attenuation coefficients of HUs and TAU-n. Thus, it may be assumed that TAU-n, which uses ultrasound waves, is able to provide an accurate representation of the degrees of mineralization and bone density in the jawbone area.

- Using the Average(log) values generated with TAU-n, we confirmed a general correspondence between HU values and R/C multiplex analysis in a cohort of 210 people with BMDJ/FDOJ patients.
- Table 1 shows two participants (#53 = 2.29 and #123 = 2.67) with an Average(log) value > 2 from the total of 210 participants.
- Here, HU values and post-operatively measured levels of cytokine expression confirm the reliability of TAU-n measurements with respect to displaying decreased bone density in cases of BMDJ/FDOJ.

LIMITATIONS

The limitations of this study include the sample size. Bias may also be present owing to the fact that not all parameters were validated in the cohort with healthy jawbone. For ethical reasons, surgical intervention and the measurement of R/C expression in healthy jawbone without any sign of BMDJ/FDOJ was not applicable.

CONCLUSION

A newly developed ultrasonography device (TAU-n) is able to detect and localize BMDJ/FDOJ caused by the fatty-degenerative dissolution of medullary trabecular structures in the jawbone. As other studies have confirmed (Guglielmi and de Terlizzi 2009; Komar et al. 2019), ultrasonography is a low-cost and efficient means of assessing jawbone health, and this was replicated with the use of the new TAU device presented here. This study established a new value using TAU-n which provides a reliable indicator of poor bone quality, rendering the device a useful tool for treatment-planning strategies in implantology as well as for fostering cooperation among professionals when assessing or treating osteoimmunologic diseases and linking such diseases with the immune system. TAU-n thus provides a non-harmful alternative to the use of X-ray irradiation, which is increasingly criticized (Brenner et al. 2001; Vañó et al. 2017), particularly in view of more stringent radiation protection laws (Strahlenschutzgesetz 1966). TAU-n represents a novel type of imaging acquisition process in dentistry and offers the ability to non-invasively assess hidden BMDJ/FDOJ in the human jawbone.

Further extensive clinical trials and multicenter comparative measurements examining TAU-n should be carried out to establish a new classification based on ultrasound and perform a reliability assessment.

Acknowledgments—English-language editing of this manuscript was provided by Journal Prep Services. Additional editing was provided by Natasha Gabriel. The practical measurements with the TAU-n were performed at our clinic by Gabriele Zidek and Tanja Scheller.

Conflict of interest disclosure—CaviTAU (Munich, Germany), the company that designed the new TAU-n apparatus and associated software, provided these tools without charge for the purposes of this study. The ultrasonography procedure was carried out at the Clinic for Integrative Dentistry (Munich, Germany). CaviTAU and the Clinic for Integrative Dentistry are engaged in ongoing discussions regarding numerous collaborative arrangements to further improve and verify the new TAU apparatus, CaviTAU, as it is introduced to the market. The corresponding author is the holder of a patent used in the CaviTAU.

REFERENCES

Al-Nawas B, Grötz KA, Kann P. Ultrasound transmission velocity of the irradiated jaw bone in vivo. Clin Oral Investig 2001;5:266–268.

Bouquot JE, Roberts AM, Person P, Christian J. Neuralgia-inducing cavitational osteonecrosis (NICO): Osteomyelitis in 224 jawbone samples from patients with facial neuralgia. Oral Surg Oral Med Oral Pathol 1992;73:307–319.

Brenner DJ, Elliston CD, Hall EJ, Berdon WE. Estimated risks of radiation-induced fatal cancer from pediatric CT. AJR Am J Roentgenol 2001;176:289–296.

Greenfield MA, Craven JD, Huddleston A, Kehrer ML, Wishko D, Stern R. Measurement of the velocity of ultrasound in human cortical bone in vivo: Estimation of its potential value in the diagnosis of osteoporosis and metabolic bone disease. Radiology 1981;138:701–710.

Guglielmi G, de Terlizzi F. Quantitative ultrasound in the assessment of osteoporosis. Eur J Radiol 2009;71:425–431.

Kaufman JJ, Einhorn TA. Ultrasound assessment of bone. J Bone Miner Res 1993;8:517–525.

Klein MO, Grötz KA, Manefeld B, Kann PH, Al-Nawas B. Ultrasound transmission velocity for noninvasive evaluation of jaw bone quality *in vivo* before dental implantation. Ultrasound Med Biol 2008;34:1966–1971.

Komar C, Ahmed M, Chen A, Richwine H, Zia N, Nazar A, Bauer L. Advancing methods of assessing bone quality to expand screening for osteoporosis. J Osteopath Med 2019;119:147–154.

Kumar VV, Sagheb K, Klein MO, Al-Nawas B, Kann PH, Kämmerer PW. Relation between bone quality values from ultrasound transmission velocity and implant stability parameters—an *ex vivo* study. Clin Oral Implants Res 2012;23:975–980.

Lechner J. Validation of dental X-ray by cytokine RANTES—comparison of X-ray findings with cytokine overexpression in jawbone. Clin Cosmet Investig Dent 2014;6:71–79.

Lechner J, Huesker K, Von Baehr V. Impact of RANTES from jawbone on Chronic Fatigue Syndrome. J Biol Regul Homeost Agents 2017;31:321–327.

Lechner J, Mayer W. Immune messengers in neuralgia inducing cavitational osteonecrosis (NICO) in jaw bone and systemic interference. Eur J Integr Med 2010;2:71–77.

Lechner J, Rudi T, von Baehr V. Osteoimmunology of tumor necrosis factor-alpha, IL-6, and RANTES/CCL5: A review of known and poorly understood inflammatory patterns in osteonecrosis. Clin Cosmet Investig Dent 2018;10:251–262.

Lechner J, Schuett S, von Baehr V. Aseptic-avascular osteonecrosis: Local "silent inflammation" in the jawbone and RANTES/CCL5 overexpression. Clin Cosmet Investig Dent 2017;9:99–109.

Lechner J, von Baehr V. Chemokine RANTES/CCL5 as an unknown link between wound healing in the jawbone and systemic disease: Is prediction and tailored treatments in the horizon?. EPMA J 2015;6:10.

Lechner J, von Baehr V. RANTES and fibroblast growth factor 2 in jawbone cavitations: Triggers for systemic disease?. Int J Gen Med 2013;6:277–290.

Lechner J, Zimmermann B, Schmidt M, von Baehr V. Ultrasound sonography to detect focal osteoporotic jawbone marrow defects: Clinical comparative study with corresponding Hounsfield units and RANTES/CCL5 expression. Clin Cosmet Investig Dent 2020;12:205–216.

Lee SC, Jeong CH, Im HY, Kim SY, Ryu JY, Yeom HY, Kim HM. Displacement of dental implants into the focal osteoporotic bone marrow defect: A report of three cases. J Korean Assoc Oral Maxillofac Surg 2013;39:94–99.

Lipani CS, Natiella JR, Greene GW, Jr. The hematopoietic defect of the jaws: A report of sixteen cases. J Oral Pathol Med 1982;11:411–416.

Loubele M, Bogaerts R, Van Dijck E, Pauwels R, Vanheusden S, Suetens P, Marchal G, Sanderink G, Jacobs R. Comparison between effective radiation dose of CBCT and MSCT scanners for dentomaxillofacial applications. Eur J Radiol 2009;71:461–468.

Mah P, Reeves TE, McDavid WD. Deriving Hounsfield units using grey levels in cone beam computed tomography. Dentomaxillofac Radiol 2010;39:323–335.

Mahmoud A, Cortes D, Abaza A, Ammar H, Hazey M, Ngan P, Crout R, Mukdadi O. Noninvasive assessment of human jawbone using ultrasonic guided waves. IEEE Trans Ultrason Ferroelectr Freq Control 2008;55:1316–1327.

Misch CE. Bone density: A key determinant for clinical success. In: Misch CE, ed. Contemporary implant dentistry. 2nd edition St Louis: CV Mosby; 1999. p. 109–118.

Njeh CF, Hans D, Fuerst T, Glüer CC, Genant HK. Quantitative ultrasound: Assessment of osteoporosis and bone status. London: Martin Dunitz; 1999.

Norton MR, Gamble C. Bone classification: An objective scale of bone density using the computerized tomography scan. Clin Oral Implants Res 2001;12:79–84.

Roberts JA, Drage NA, Davies J, Thomas DW. Effective dose from cone beam CT examinations in dentistry. Br J Radiol 2009;82:35–40.

Strahlenschutzgesetz (StrlSchG) Artikel 1 G. v. 27.06.2017 BGBl. I S. Strahlenschutzverordnung (StrlSchV) Artikel 1 V. v. 29.11.2018 BGBl. I S. 2034, 2036. Gesetz zur Neuordnung des Rechts zum Schutz vor der schädlichen Wirkung ionisierender Strahlung (StrlSchGEG) G. v. 27.06.2017 BGBl. I S. 1966. .

Swennen GRJ, Schutyser F. Three-dimensional cephalometry: Spiral multi-slice vs cone-beam computed tomography. Am J Orthod Dentofacial Orthop 2006;130:410–416.

Vañó E, Miller DL, Martin CJ, Rehani MM, Kang K, Rosenstein M, Ortiz-López P, Mattsson S, Padovani R, Rogers A. Authors on behalf of ICRP. ICRP publication 135: Diagnostic reference levels in medical imaging. Ann ICRP 2017;46:1–144.

Wells PNT. Ultrasonic imaging of the human body. Rep Prog Phys 1999;62:671.